Applied Water Science (2024) 14:153
https://doi.org/10.1007/s13201-024-02191-6

ORIGINAL ARTICLE

'Off–On' determination of lead (Pb^{2+}) and fluoride (F^{-}) ion in fish and wastewater samples using N, S co-doped carbon quantum dots (N, S-CQDs)

Olanrewaju Aladesanmi Aladesuyi[1,2] · **Oluwatobi Samuel Oluwafemi**[1,2]

Received: 29 November 2023 / Accepted: 22 April 2024 / Published online: 8 June 2024

Abstract
Lead is a global priority pollutant. Its presence in aquatic systems is harmful to the human health. Fluoride is essential to the human body, especially in dental health. However, excess fluoride in the body can lead to serious health concerns. Therefore, a simple approach to monitoring lead and fluoride in environmental samples is paramount. In this study, we synthesized N and S co-doped carbon quantum dots under the hydrothermal method by employing citric acid, glutamine, and sodium sulphide (Na_2S) as precursors. Characterization of the developed nanosensor was carried out using Fourier transform infrared spectroscopy (FTIR), high-resolution transmission electron microscopy (HRTEM), photoluminescence (PL) spectrophotometer, ultraviolet–visible spectroscopy (UV–Vis), and X-ray diffraction (XRD). The as-prepared nanosensor is spherical with an average particle diameter of 3.45 ± 0.86 nm and emits light in the green region of the spectrum. This material was employed as an 'on–off' and 'off–on' fluorescent sensor to determine Pb^{2+} and F^{-} rapidly and selectively. The fluorescence was quenched (turned off) in the presence of Pb^{2+} because of the strong interaction between Pb^{2+} ions and the surface functional groups of the as-synthesized material. Subsequently, the quenched fluorescence of the N, S-CQDs + Pb^{2+} system was restored (turned on) upon the introduction of F^{-} ions, owing to the formation of ionic bonds between Pb^{2+} and F^{-}. The N S-CQDs were selective towards Pb^{2+}. At the same time, the N, S-CQDs + Pb^{2+} system exhibited selectivity towards F^{-} ions amidst other ions with low detection limits (LODs) of 13.35 nM and 43.17 nM for Pb^{2+} and F^{-}, respectively. The dynamic quenching mechanism was suggested based on the absorption spectra and lifetime results. Satisfied recoveries of 89.30–116.40% for Pb^{2+} and 90.22–115.05% for F- (RSD < 5) were obtained in practical samples of wastewater and fish. We believe that the as-synthesized N S-CQDs can effectively serve as reliable, accurate, and swift nanosensor for detecting Pb^{2+} and F^{-} in environmental samples.

Keywords Carbon quantum dots · Fluorescent recovery · Waste water · Pb^{2+} · F^{-} · Green emission

Introduction

Lead is a significant water pollutant. Lead in aquatic systems is harmful and injurious to human health and well-being. Industries such as battery manufacturing, lead-tetra acetyl, ceramic processing, and iron smelting, to mention a few, are significant examples of sectors that disperse lead-polluted water into water bodies (Chooto 2020). In the list of priority pollutants, lead had been categorized as priority number two according to the Agency for Toxic Substances and Disease Registry (ATSDR) (United States Environmental Protection Agency 2021). Lead has little biodegradability and is highly soluble in water, thereby increasing the risk of absorption by living organisms, especially seafood, and subsequently into human systems through ingestion of seafood (Kinuthia et al. 2020; Vardhan et al. 2019). Lead exposure can damage the brain and central nervous system, causing coronary heart disease, coma, and even death. In children, exposure to lead can cause permanent intellectual disability and disordered behaviour. Fluoride ion, in the right amount, is essential in potable water. The presence of fluoride in water prevents

✉ Oluwatobi Samuel Oluwafemi
Oluwafemi.oluwatobi@gmail.com

[1] Department of Chemical Sciences, University of Johannesburg, P.O. Box 17011, Doornfontein 2028, Johannesburg, South Africa

[2] Centre for Nanomaterials Science Research, University of Johannesburg, Johannesburg, South Africa

tooth decay and the formation of cavities. At the same time, excess fluoride can lead to health issues such as dental fluorosis, brain impairment, and nervous system disorder. Industries that produce glass, fertilizer, semiconductors, and precious metals require fluoride as a processing chemical.

The availability of potable water is a global challenge; about one-third of the world's population accesses drinking water through rivers, lakes, streams, and canals. The primary cause of water pollution is the discharge of untreated or inadequately treated industrial effluents into surface water. In developing countries, most wastewater is not treated before being released into water bodies. Sadly, most of the population in developing countries still rely on untreated surface water as their primary source of domestic water. Chances are high that wastewater from such industries will contain fluoride pollutants (El Diwani et al. 2022; Wang et al. 2021). Fluoride ion has been described as a significant source of groundwater pollution (Duggal et al. 2022; Podgorski et al. 2022).

Therefore, the need to adequately monitor the level of Pb^{2+} and F^{-} priority pollutants in wastewater, seafood, and the environment is of utmost importance to the well-being of humans. Traditional analytical methods have been employed to determine Pb^{2+} and F^{-} (Gao et al. 2015; Sisay et al. 2019; Zhang et al. 2017). Despite the reliability and sensitivity of these techniques, disadvantages exist, such as expensive operation costs, tedious procedures, and complex and time-consuming sample preparation. Hence, exploring other cheaper, more rapid, and sensitive methods for detecting Pb^{2+} and F^{-} is inevitable.

Recently, the use of carbon quantum dots as a nanoprobe for metal ion sensing and other applications has garnered widespread interest because of their superior properties such as, cost-effectiveness and facile synthetic methods, photostability, non-toxic nature, and biocompatibility, to mention a few (Atabaev et al. 2018; Yoo et al. 2019). Numerous methods have been employed in the synthesis of carbon quantum dots (CQDs); they include electrochemical synthesis (An et al. 2021), microwave-assisted (de Medeiros et al. 2019), hydrothermal (Zhu et al. 2022), pyrolysis carbonation method (Ye et al. 2017), etc. However, the hydrothermal technique provides the following merits: ease of operation, eco-friendliness, and the CQDs obtained are mono-dispersible (Shabbir et al. 2021; Yadav et al. 2023). Several approaches have been utilized to improve CQDs fluorescence performance and optical properties, including doping or co-doping with metal and non-metallic heteroatoms. However, metallic doping or co-doping has been discouraged mainly due to the toxicity and non-uniformity of the metallic dopant.

Consequently, non-metallic heteroatoms such as nitrogen, sulphur, and phosphorus have been widely applied as dopants or co-dopants in the synthesis of CQDs for metal ion detection (Chaghaghazardi et al. 2023; Mohandoss et al. 2023; Pei et al. 2023; Yang et al. 2018). As indicated by numerous reports, co-doping with N and S is the most intriguing form of doping. Co-doping with these two results in improved quantum yield, fluorescent intensity, and red shift in emission wavelength (Sarkar et al. 2016). Three sensing strategies are involved in using CQDs for the fluorescent detection of analytes (Kainth et al. 2022). They are (i) direct interaction between the analyte and the CQDs leading to a change in fluorescence (Aladesuyi and Oluwafemi 2023a), (ii) post-synthesis functionalization of the CQDs through conjugation with specific receptors to ensure selective and sensitive fluorescent response of the analyte (Zou et al. 2020), and (iii) combination of CQDs with a sensory material that acts as a fluorescent quencher which can interact with the target analyte and lead to fluorescent recovery (Bai et al. 2021). In this study, the principles of quenching and fluorescence recovery were employed to create a nanoprobe for identifying and measuring Pb^{2+} and F^{-} in wastewater and fish species. Analyte detection via luminescence 'off–on' technique using CQDs has been reported (Raja et al. 2023; Li et al. 2021). Boruah et al. (2020) developed a CQDs fluorescent probe for detecting Eu^{3+} and F^{-} via an 'off–on' using biomass waste material as the precursor. The luminescence of the developed CQDs was quenched (off) upon adding Eu^{2+} and restored (on) when F^{-} was introduced. The as-synthesized nanoprobe was sensitive and selective in detecting F^{-} in aqueous solution. In another study, Liu et al. (2022) developed an 'on–off' and 'off–on' fluorescence nanoprobe for the detection and quantification of Hg^{2+} and I^{-} using polyethyleneimine and anhydrous citric acid as precursors. The obtained nanoprobe selectively detected Hg^{2+} and I^{-} in river water with low detection limits and satisfactory accuracy. To the best of our knowledge, the determination of Pb^{2+} and F^{-} in wastewater and consumed fish using nanoprobe such as CQDs has not been reported.

In this work, N,S-CQDs was synthesized hydrothermally using citric acid, glutamine, and sodium sulphide as precursors. The photostability of the as-produced nanosensor was examined through continuous exposure to UV light. After 6 h of constant exposure, the change in the fluorescent intensity was insignificant, indicating that the material is photostable. We subsequently assessed the selectivity of the nanosensor towards Pb^{2+}. The as-synthesized nanosensor displayed excellent selectivity for Pb^{2+} amidst interfering ions. The N, S-CQDs/ Pb^{2+} complex was used as a nanoprobe for detecting F^{-} ions. The developed nanosensor was further used for measuring the amount of Pb^{2+} and F^{-} in wastewater and fish species through the 'turn off' and 'turn on' effects. Satisfactory recoveries of (89.30–116.40%) and (90.22–115.05%) were obtained for Pb^{2+} and F^{-}, respectively. The method is facile, and the developed nanoprobe can rapidly detect Pb^{2+} and F^{-} in environmental samples.

Material and methods

Materials and reagents

Citric acid, Na_2S, glutamine, H_2SO_4, n-butanol, NaOH, $PbCl_2$, $Cr(NO)_3$, $Fe(NO)_3$, $Co(NO)_3$, $Cd(NO)_3$, $Zn(NO)_3$, and $Pb(NO)_3$ were acquired from Sigma-Aldrich. Wastewater was collected from the Johannesburg canal, while Tilapia fish were procured in Johannesburg at the Shoprite supermarket. There was no further purification of the purchased materials.

Synthesis of N,S-CQDs

The co-doped CQDs were synthesized following our previous report with slight modifications (Aladesuyi and Oluwafemi 2023b). Citric acid (6mmoles), glutamine (9mmoles), and Na_2S (9mmoles) were dissolved in 30 mL of deionized water. A homogenous mixture was obtained by slight stirring and ultrasonication at room temperature. Subsequently, this resulting mixture was placed in a Teflon-lined stainless-steel autoclave and heated at 200 °C for 3 h. Upon cooling, the obtained yellowish solution underwent centrifugation for 15 min at 10,000 rpm and filtered through a 0.02-µm filter paper to eliminate any unreacted particles. Dissolved impurities were removed by washing the solution severally with n-butanol. Afterwards, solid crystals of the developed nanosensor were obtained after freeze-drying.

Characterization of N,S-CQDs

The characterisation of the as-synthesized material was achieved using different techniques, which include JOEL (JEM 2100) high-resolution transmission electron microscope (HRTEM) for the morphology and particle size, Spectrum Two PerkinElmer Fourier transform infrared instrument (FTIR) fitted with an attenuated total reflection sample holder with a scanning range of 400–4000 cm^{-1} for the surface chemistry. An FS5 spectrofluorometer (Edinburg instrument) was used for lifetime and fluorescence measurement using a 1-cm quartz cuvette at λ_{ex} of 460 nm. The excitation and emission slit were set at 5 nm, with a visible PMT-980 detector. The data were processed using Flouracle software. A double-beam SP-UV 500 spectrophotometer (Perkin Elmer) was used for absorption spectra measurement, while Brucker D8 advance diffractometer with monochromatic $CuK_{\alpha 1}$ radiation ($\lambda = 1.5418$ Å) was used for XRD analysis.

Fluorescent detection of Pb^{2+} and F^-

The following procedure was followed for the fluorescent detection of Pb^{2+}: 100 µL of the nanosensor was introduced into a cuvette containing 3 mL of water and the fluorescence was measured at an excitation wavelength of 460 nm. The sensitivity was determined by placing the developed nanosensor individually in separate cuvettes, each containing 100 µM of various metal salts, including $Zn(NO_3)_2$, $Co(NO_3)_2$, $Pb(NO_3)_2$, $Cr(NO_3)_3$, $Cd(NO_3)_2$, NaCl, KCl, and $Fe(NO_3)$. The spectrofluorometer was used to record the fluorescence of the respective nanosensor/metal ion mixtures, and the fluorescent responses were compared. Subsequently, the fluorescent spectra of the nanosensor amidst various Pb^{2+} standards were recorded. To investigate the selectivity of the developed material towards Pb^{2+}, the fluorescent spectra of a mixture containing the nanosensor, Pb^{2+}(100 µM), along with the same volume and concentration of each of the individual metal ions such as Co^{2+}, Cd^{2+}, Fe^{3+}, Cr^{3+}, Zn^{2+}, Na^+, and K^+ were recorded under the same experimental conditions.

For F^- ion detection, N, S-CQDs solution (100 µL) and Pb^{2+} solution (3 mL, 100 µM) were added in a centrifuge tube. The N, S-CQDs/Pb^{2+} mixture was combined with various concentrations of F^- standards, and the total volume was adjusted to 3 mL. Subsequently, fluorescent spectra were recorded under the same conditions employed to determine Pb^{2+}. In evaluating the selectivity of the N, S-CQDs/Pb^{2+} nanoprobe towards F^-, the fluorescence response of a mixture of F^- (100 µM), along with the same volume and concentration of anions such as Cl^-, Br^-, I^-, CO_3^{2-}, PO_4^-, NO_3^-, was recorded under the same experimental conditions.

Actual sample analysis

The detection of Pb^{2+} and F^- in Tilapia fish extracts and environmental wastewater was performed to determine the reliability and precision of the developed sensor in the actual sample. The preparation of fish extracts was carried out using our previously reported method (Aladesuyi and Oluwafemi 2023b). The wastewater samples were obtained from the Johannesburg canal and filtered using 0.22-µm filter paper to remove insoluble waste materials. To detect Pb^{2+} in the resultant solutions, each sample solution, consisting of 3 mL, was combined with 100 µL of the prepared nanosensor in a cuvette, and their photoluminescence was recorded at 460 nm excitation.

Results and discussion

Characterization and optical properties of N,S-CQDs

The structural and morphological properties of the synthesized N,S-CQDs were examined using HRTEM, FTIR, and XRD techniques. HRTEM analysis (Fig. 1a) revealed that the developed nanosensor exhibited uniform dispersion and a quasi-spherical shape with an average particle diameter of 3.45 ± 0.86 nm. The crystalline nature of the material was confirmed by the presence of lattice fringes with a measured lattice spacing of 0.23 nm, matching the (002) lattice planes of graphite.

XRD analysis (Fig. 1b) showed a broad hump at $2\theta = 21.55°$, corresponding to the (002) graphite lattice plane, indicating a low graphitic carbon structure. The FTIR spectrum (Fig. 1c) shows a peak at 3214 cm^{-1} attributed to O–H stretching vibration bands from the carboxylic groups on the surface of the N,S-CQDs, while the peak at 3096 cm^{-1} corresponded to the N–H stretching from the conjugated amide group. The absorption bands at 1661 cm^{-1} and 1576 cm^{-1} represented the C = O and C-NH groups, respectively. The peak at 713 cm^{-1} confirmed the presence of C-S stretching vibrations (Wu and Tong 2019), while

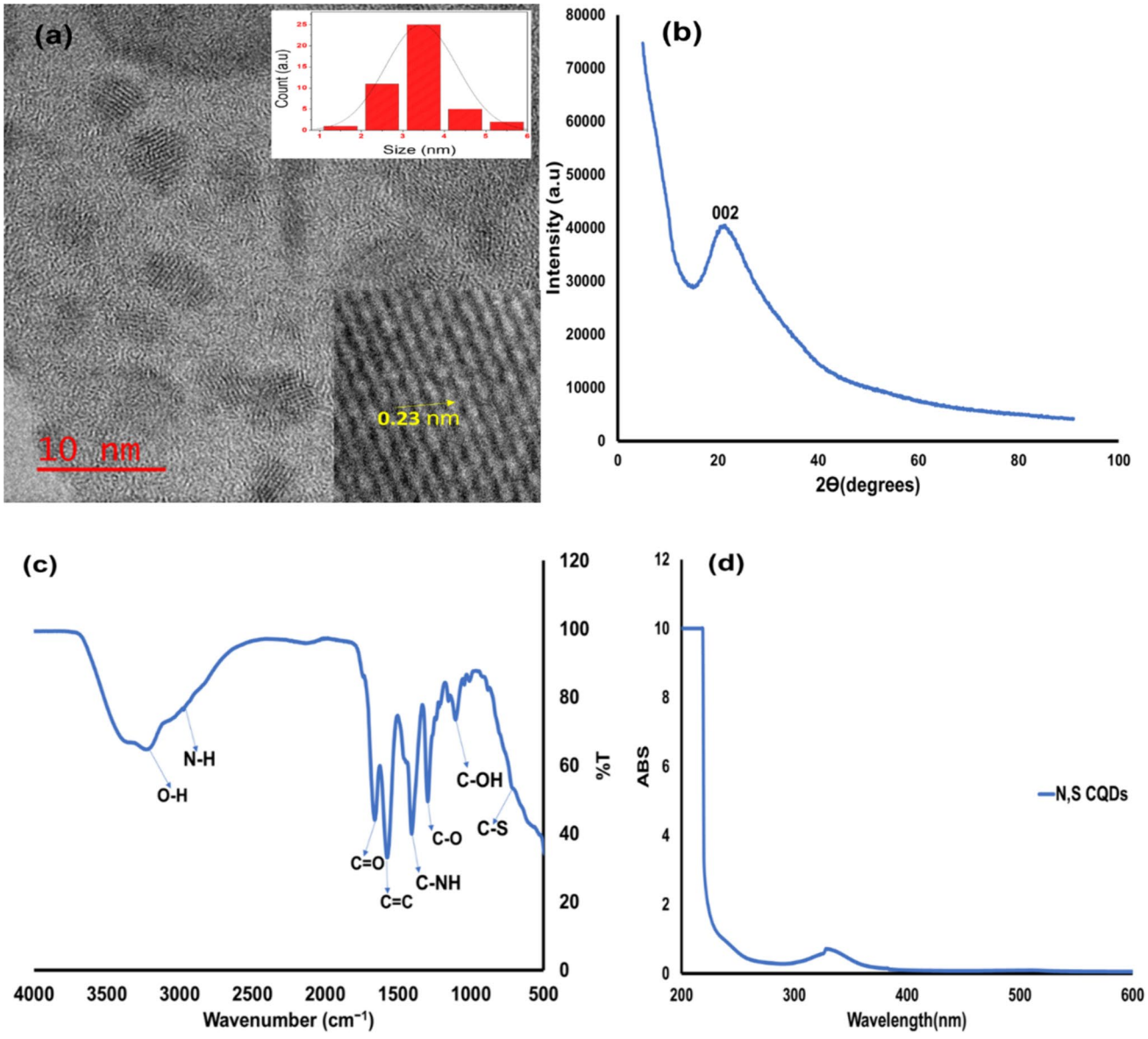

Fig. 1 **a** TEM micrograph (inset: size distribution and lattice fringes) and **b** XRD pattern **c** FTIR spectrum and **d** Absorption spectrum of the N,S-CQDs

the peaks in the range of 1406–1102 cm^{-1} were assigned to C–C, C–N, and C–O stretching vibration bands. The existence of these hydrophilic groups on the CQDs' surface likely contributed to their improved solubility and fluorescence behaviour (Zu et al. 2017).

The optical properties of the synthesized nanosensor were explored through UV–Vis absorption and photoluminescence spectroscopy (Fig. 1d). The absorption spectra exhibited two peaks at 225 and 330 nm. The former corresponded to the π–π* transition of aromatic C = C and C = N bonds, while the latter could be attributed to the n-π* transition of the C = O bond (Hao et al. 2023; Keenan et al. 2019). The quantum yield (QY) significantly increased from 1.59 to 10.35% when co-doping with N and S, indicating that co-doping with electron-rich heteroatoms substantially enhanced the QY. The N,S-CQDs exhibited excitation-dependent emission, a phenomenon influenced by the energy state at the surface (Hu 2016).

Fluorescent detection of Pb^{2+}

The ability of the N,S-CQDs to accurately detect Pb^{2+} was investigated under optimized experimental parameters at pH 6 and an incubation time of 5 min to ensure proper interaction between the nanosensor and the quencher molecule (Pb^{2+}). The fluorescent intensity of the as-prepared material decreased gradually in the presence of Pb^{2+} standards. The degree of reduction in fluorescent intensity was concentration-dependent (Fig. 2a). The decrease in fluorescent intensity had been attributed to the coordination of the Pb^{2+} ion with the carboxyl or sulfhydryl group on the CQDs' surface (Dewangan et al. 2022; Shi et al. 2022). The formation of complexes involving metal ions, hydroxyl, and carboxyl groups gives rise to changes in the electronic structure of the N, S-CQDs, which, in turn, disrupts the activity and arrangement of the electrons. This adjustment in electron distribution can lead to non-radiative recombination of electrons and holes and, consequently, a reduction in the fluorescent intensity of the CQDs. The reduced fluorescent intensity at different Pb^{2+} standards (0 to 25 µM) has a linear relationship, as illustrated in Fig. 2b. This linear correlation conforms to the Stern–Volmer equation, with an R^2 value of 0.9913.

$$\frac{Fo}{F} = K_{sv}C + 1$$

K_{sv}—Stern–Volmer constant, C—concentration of quencher ion (Pb^{2+}), F and F_o are the respective PL intensities of nanosensor with and without Pb^{2+} ions.

The calculated limit of detection (LOD) of 13.13 nM was obtained based on $\frac{3SD}{S}$ (SD is the standard deviation, S is the slope of the calibration curve). The as-synthesized material can detect Pb^{2+} with selectivity and sensitivity comparable to previous reports (Table 1).

Sensors' selectivity and anti-interference ability are vital tools in determining the efficacy and suitability of the material, especially their potential applications in complex systems. As a result, common metal ions such as Co^{2+}, Cd^{2+}, Fe^{3+}, Cr^{3+}, Zn^{2+}, Na^{+} and K^{+} were used in investigating the selectivity (Fig. 2c) and the anti-interference (Fig. 2d) ability of the as-synthesized nanosensor. The result shows that the presence of the other metal ions has little or no impact on the fluorescence response of the nanosensor to Pb^{2+}. This indicates that the as-synthesized material is highly selective towards Pb^{2+} ions compared to other interfering ions.

Fluorescent detection of F^- using N,S-CQDs-Pb^{2+} nanoprobe

The affinity between lead and fluoride motivates the design of an 'off–on' fluorescent nanoprobe for the determination of fluoride in actual samples. The ability of the N, S-CQDs-Pb^{2+} to detect F^- was investigated by adding fluoride standards (0-12 µM) under optimized experimental conditions (pH 6 and incubation time of 5 min) at 460 nm excitation. The result (Fig. 3a) indicates that the as-synthesized nanosensor transited from the 'off' mode due to the quenching effect of Pb^{2+} to the 'on' mode (fluorescence recovery) due to F^- standards. The extent of fluorescent recovery is concentration-dependent, a clear indication that the N,S-CQDs-Pb^{2+} can be used to detect and quantify F^-. The fluorescent recovery could be attributed to the ionic bond formation between lead and fluoride to give PbF_2. In addition, lead, a relatively hard acid, will have an affinity for a hard base in water, such as fluoride ions. The linear relationship between the change in fluorescent intensity and F^- standards (0–12 µM) is shown in Fig. 3b; the detection limit was calculated to be 43.17 nM. The selectivity studies (Fig. 3c) show that the N-S-CQDs + Pb^{2+} system was selective towards F^- compared to other non-metal ions tested (Cl^-, Br^-, I^-, CO_3^{2-}, NO^-_3, PO^{3-}_4). There was no significant recovery in PL intensity in the presence of other anions. Furthermore, a mixture of F^- and these anions was added to the solutions of the N-S-CQDs + Pb^{2+} system under the same experimental conditions (Fig. 3d). The PL recovery was similar to that obtained using F^- ion alone as the interfering ions posed only insignificant change in the intensity of the recovered fluorescence. The result shows that the as-synthesized N-S-CQDs + Pb^{2+} nanosensor displayed an outstanding selectivity towards F^- ion in the presence of interfering ions. A comparison of various nanosensors for determining F^- ion is shown in Table 2.

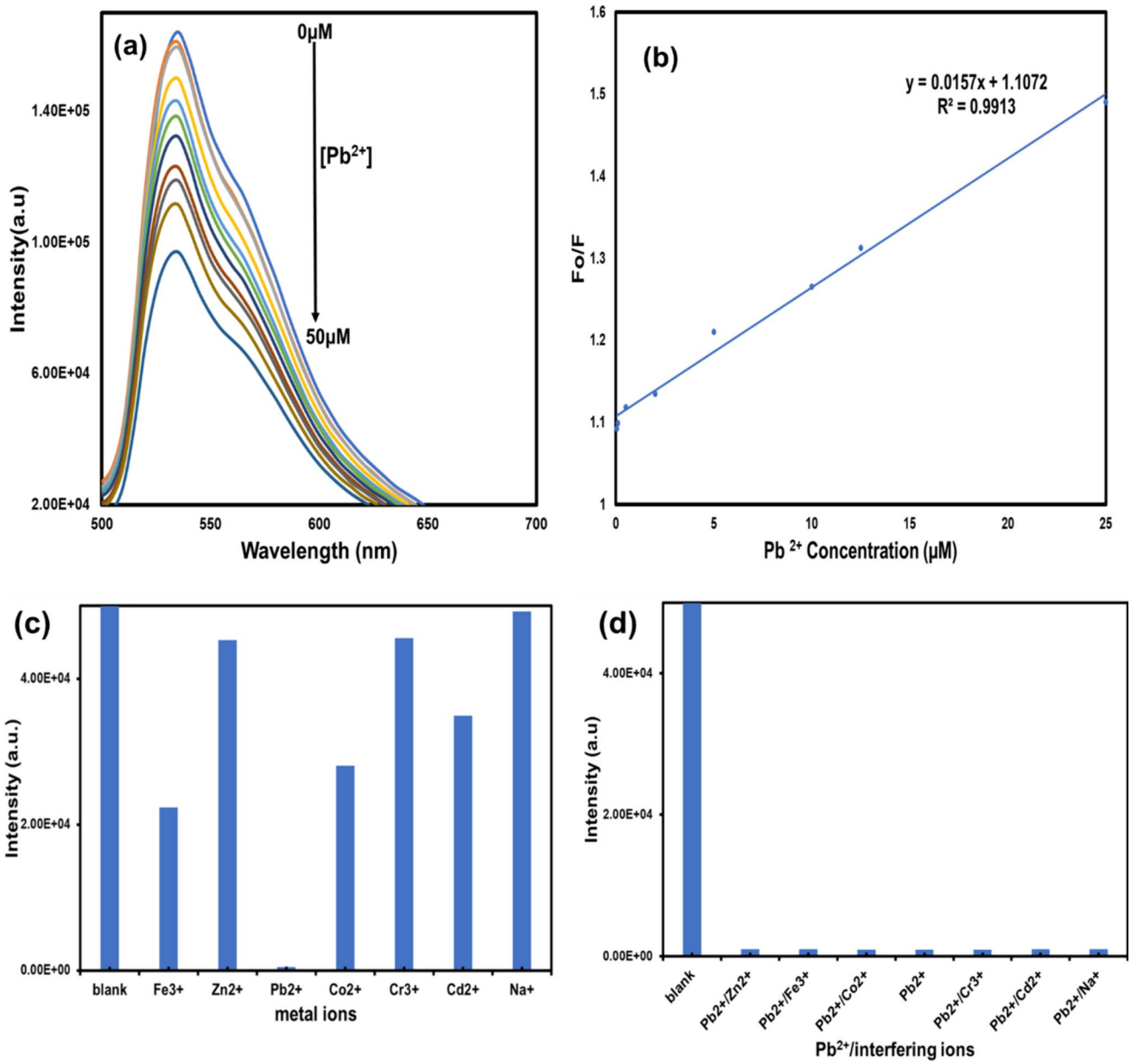

Fig. 2 **a** PL spectra of N,S-CQDs in the presence of Pb^{2+} standards and **b** Stern–Volmer plot ($R^2 = 0.9913$). Selectivity assessment of fluorescence response of the nanosensor towards Pb^{2+} **c** and metal ions **d** amid interfering metal ions

Table 1 Comparison of the as-synthesized fluorescent probe with reported methods for the detection of Pb^{2+}

Nanosensor	Precursor of CQDs	LOD (nM)	Refs
N, S-CQDs	Tri-ammonium citrate and thiourea	9.2	(Aboobakri et al. 2023)
Copper nanoclusters@N-CQDs	Sodium citrate and NH_4Cl	15	(Li et al. 2020)
N-CQDs	Ethylene glycol and NH_4OH	24.12	(Wongsing et al. 2023)
N-CQDs	Chocolate	12.7	(Liu et al. 2016)
N,S-CQDs	L-cysteine	Not given	(Gao et al. 2020)
N,S-CQDs	Citric acid, glutamine, Na_2S	13.35	This work

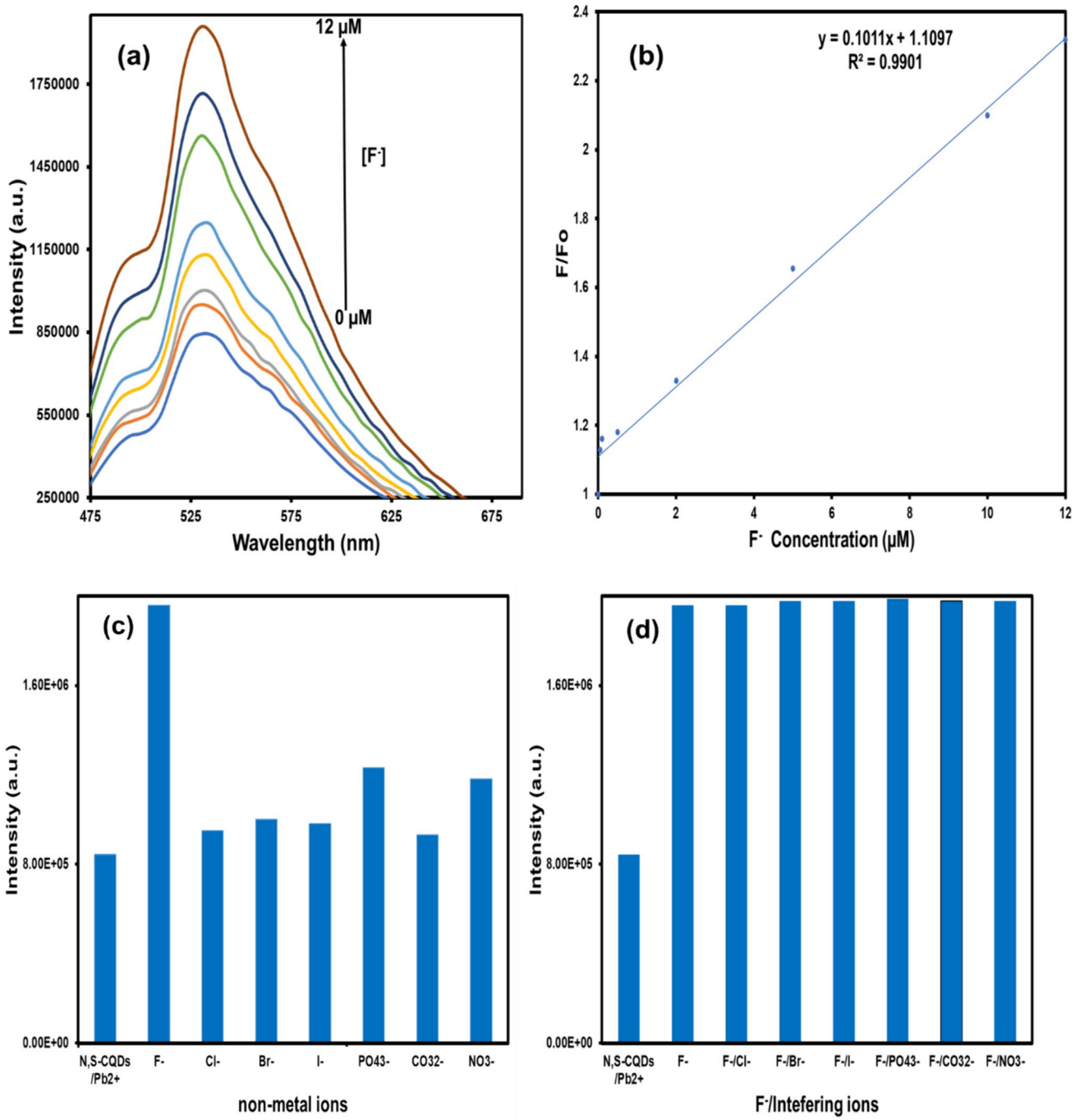

Fig. 3 **a** PL spectra of N,S-CQDs/ Pb^{2+} under the influence of F^- standards and **b** Stern–Volmer plot ($R^2 = 0.9913$). Selectivity assessment of fluorescence response of the nanosensor towards F^- **c** and non-metal ions **d** amid interfering non-metal ions

Table 2 Comparison of the as-synthesized fluorescent probe with reported methods for the detection of F^-

Nanosensor	Precursor of CQDs	LOD (nM)	Refs
CDs + Fe^{3+}	Polyvinylpyrrolidone	Approx. 1000	(Sarkar et al. 2019)
Se,N-CDs + curcumin	2,3-Diaminopyridine and selenourea	390	(Zhang et al. 2021)
CQDs + Eu^{3+}	Sugar bagasse, Taro peels and garlic peels	Not given	(Boruah et al. 2020)
CQDs + Eu^{3+}	citric acid	Not given	(Singhal et al. 2017)
Fe_3O_4@SiO_2CDs	Orange juice	60	(Mohapatra et al. 2015)
N,S-CQDs/Pb^{2+}	Citric acid, glutamine, Na_2S	43.17	This work

Detection mechanism

The common fluorescent quenching mechanisms associated with CQDs include static quenching, dynamic quenching, inner field effect (IFE), and Forster energy resonance transfer (FRET) (Tian et al. 2023; Wang et al. 2022). Static quenching occurs due to the formation of a non-fluorescent ground-state complex between the quencher and the CQDs, thereby forming a new substance (Giordano et al. 2023). Dynamic quenching, on the other hand, occurs when the CQDs return to the ground state from the excited state due to collision with the quencher molecule (Molaei 2020). This is achieved via energy or charge transfer between the duo. In FRET, the quenching mechanism occurs via energy transfer from a luminescent donor to an acceptor when the distance is within 10 nm (Gopal et al. 2024; Miao et al. 2020). This results in the donor's fluorescence loss and the enhancement of the acceptor's fluorescence. The IFE mechanism occurs when an overlap occurs between the acceptor's absorption spectrum and the CQD's excitation or emission spectra (Molaei 2020; Rahal et al. 2021). Time-resolved fluorescence lifetimes measurement and the UV absorption spectra are essential tools used to evaluate the quenching mechanism of CQD-based nanoprobe (Liu et al. 2021; Liu et al. 2024). The fluorescence lifetime and the absorption spectra of N, S-CQDs, N, S-CQDs + Pb^{2+}, and N, S-CQDs + Pb^{2+} + F^- are shown in Fig. 4a and b. The average lifetimes of N, S-CQDs, N,S-CQDs + Pb^{2+}, and N,S-CQDs + Pb^{2+} + F^- were measured to be 3.605 ns, 5.495 ns, and 5.105 ns, respectively (Fig. 4a). The lifetime increased on the addition of Pb^{2+} and F^-; the difference in the lifetime is an indication of excited state electron or energy transfer between the N,S-CQDs and the quencher molecules (Pb^{2+}), a characteristic of dynamic quenching (Long et al. 2021; Molaei 2019). The strong interaction between Pb^{2+} and F^- led to the displacement of Pb^{2+} from the surface of the N,S-CQDs, consequently leading to the recovery of fluorescent intensity. As depicted in Fig. 4b, no new absorption peaks were observed in the UV absorption spectra of N,S-CQDs, N,S-CQDs + Pb^{2+}, and N,S-CQDs + Pb^{2+} + F^-. This indicates that no new substance was formed, as there was no ground-state interaction between the nanosensor and the quencher molecules; this further suggested a dynamic quenching mechanism.

Validation of method using real samples

Wastewater and fish samples were used to determine the viability of the as-synthesized nanosensor for detecting Pb^{2+} and F^- in real samples (Table 3). Spiked samples displayed excellent recoveries with the nanosensor. Actual spiked samples showed remarkable recoveries for both Pb^{2+} (89.30%-116.40%) and F^- (90.22–115.05%) with low RSD (< 5). These results demonstrated that the developed

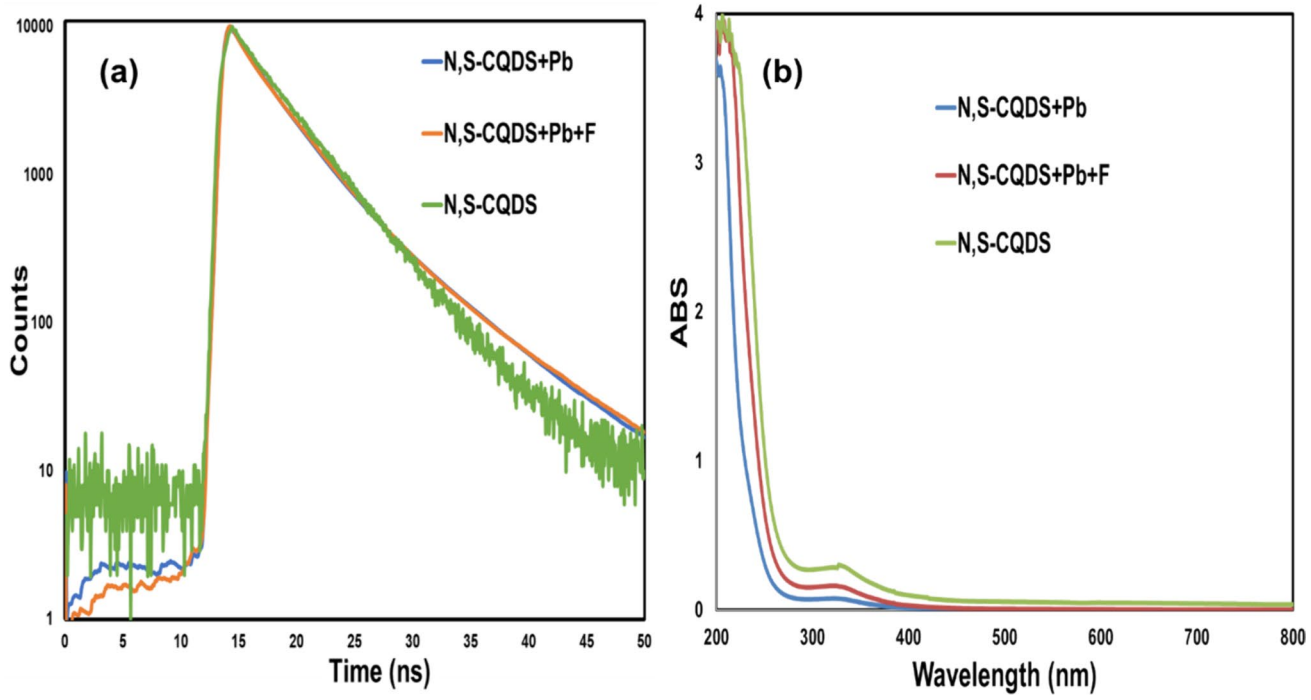

Fig. 4 **a** Fluorescence lifetime decay curve of N,S-CQDs, N,S-CQDs + Pb^{2+} and N,S-CQDs + Pb^{2+} + F^-. **b** Absorption spectra of N,S-CQDs, N,S-CQDs + Pb^{2+} and N,S-CQDs + Pb^{2+} + F^-

Table 3 Determination of Pb^{2+} and F^- in spiked samples of wastewater and fish extract using the developed nanosensor

Sample	Spiked (μM)	Pb^{2+} found (μM)	Recovery (%)	RSD (%) ($n=3$)	F^-found (μM)	Recovery (%)	RSD (%) ($n=3$)
Waste	0	ND	–	–	–	–	–
water	0.1	0.116	116.40	1.75	0.115	115.05	3.9
	0.3	0.284	94.71	2.26	0.271	90.22	2.7
	0.5	0.558	111.76	2.98	0.466	93.13	3.5
Fish	0	ND	–	–	–	–	–
Extract	0.1	0.089	89.30	4.25	0.093	92.76	3.8
	0.3	0.2905	96.86	3.97	0.278	92.51	2.8
	0.5	0.458	91.66	3.55	0.459	91.78	4.3

ND—not determined

RSD—relative standard deviation

turn 'off–on' fluorescent nanosensor is reliable and accurate for quantifying Pb^{2+} and F^- in aquatic systems.

Conclusions

In summary, we synthesized N- and S-doped carbon quantum dots using CA, glutamine, and Na_2S as precursors through a facile hydrothermal method. The resulting nanosensor was employed as an 'on–off' and 'off–on' fluorescent sensor for precisely detecting Pb^{2+} and F^- ions with outstanding sensitivity and selectivity. A LOD of 13.35 nM and 43.17 nM was obtained for Pb^{2+} and F^-, respectively. The quenching mechanism, as evidenced by fluorescence decay lifetime and UV–Vis spectrum analysis, indicated a dynamic quenching mechanism. Furthermore, this developed material was effectively employed as a fluorescent probe for detecting Pb^{2+} and F^- ions in wastewater and fish samples, respectively, yielding accurate measurements and excellent recovery rates. Thus, the developed nanosensor is a promising tool for the rapid assessment of Pb^{2+} and F^- ions in aquatic systems. Based on this study and previous literature, CQD-based nanosensors have shown exemplary performance regarding accuracy, selectivity, and low LODs. However, performance improvement in specific areas, such as longer wavelength emission and higher fluorescent quantum yield, still needs to be achieved. In addition, the design of CQDs that will be useful for adequately sensing gaseous pollutants is highly desirable.

Acknowledgements We express our gratitude to the National Research Foundation (N.R.F.) for their support through the Competitive Programme for Rated Researchers (CPRR), Grants No. 129290. Additionally, University of Johannesburg (U.R.C.) and the Faculty of Science (F.R.C.) for the financial assistance provided.

Declarations

Conflict of interest The authors declare no known conflict of interest.

Ethical approval This research does not involve using human participants or any life animal. The fish extract used in the study was obtained in the supermarket, which was edible and meant for consumption.

References

Aboobakri E, Heidari T, Jahani M (2023) N, S co-doped fluorescent carbon dots synthesized by microwave irradiation: a sensitive probe for Pb (II) ions detection in food samples. Carbon Lett 33:1629–1638. https://doi.org/10.1007/s42823-023-00529-9

Aladesuyi OA, Oluwafemi OS (2023a) Synthesis of glutamine-based green emitting carbon quantum dots as a fluorescent nanoprobe for the determination of iron (Fe^{3+}) in Solanum tuberrosum (potato). Heliyon 9(5):e15904

Aladesuyi OA, Oluwafemi OS (2023b) Synthesis of N, S co-doped carbon quantum dots (N, S-CQDs) for sensitive and selective determination of mercury (H^{g2}+) in Oreochromis niloctus (Tilapia fish). Inorganic Chem Comm 153:110843. https://doi.org/10.1016/j.inoche.2023.110843

An Q, Lin Q, Huang X, Zhou R, Guo X, Xu W, Wang S, Xu D, Chang H (2021) Electrochemical synthesis of carbon dots with a Stokes shift of 309 nm for sensing of Fe^{3+} and ascorbic acid. Dyes Pigm 18:108878. https://doi.org/10.1016/j.dyepig.2020.108878

Atabaev TS (2018) Doped carbon dots for sensing and bioimaging applications: a minireview. Nanomaterials 8(5):342. https://doi.org/10.3390/nano8050342

Bai Y, Zhao J, Wang S, Lin T, Ye F, Zhao S (2021) Carbon dots with absorption Red-shifting for two-photon fluorescence imaging of tumor tissue pH and synergistic phototherapy. ACS Appl Mater Interfaces 13:30. https://doi.org/10.1021/acsami.1c08076

Boruah A, Saikia M, Das T, Goswamee TL, Saikia BK (2020) Blue-emitting fluorescent carbon quantum dots from waste biomass sources and their application in fluoride ion detection in water. J Photochem Photobiol B 209:111940. https://doi.org/10.1016/j.jphotobiol.2020.111940

Chaghaghazardi M, Kashanian S, Nazari M, Omidfar K, Joseph Y, Rahimi P (2023) Nitrogen and sulfur co-doped carbon quantum dots fluorescence quenching assay for detection of mercury (II). Spectrochim Acta A Biomol Specrtosc 293:1386–1425. https://doi.org/10.1016/j.saa.2023.122448

Chooto P (2020) Lead chemistry. IntechOpen. https://doi.org/10.5772/intechopen.87761

De Medeiros TV, Manioudakis J, Noun F, Macairan J, Victoria F, Naccache R (2019) Microwave-assisted synthesis of carbon dots and their applications. J Mater Chem C 7:7175–7195. https://doi.org/10.1039/C9TC01640F

Dewangan L, Chawre Y, Korram J, Karbhal I, Nagwanshi R, Jain V, Satnami ML (2022) N-doped, silver, and cerium co-doped carbon quantum dots based sensor for detection of Hg^{2+} and captopril. Microchem J 182:107867a. https://doi.org/10.1016/j.microc.2022.107867

Duggal V, Sharma S (2022) Fluoride contamination in drinking water and associated health risk assessment in the Malwa Belt of Punjab. India Environ Adv 8:100242. https://doi.org/10.1016/j.envadv.2022.100242

El Diwani G, Amin SK, Attia NK, Hawash SI (2022) Fluoride pollutants removal from industrial wastewater. Bull Natl Res Cent 46:143. https://doi.org/10.1186/s42269-022-00833-w

Gao Y, Xu M, Sturgeon RE, Mester Z, Shi Z, Galea R, Saull P, Yang L (2015) Metal ion-assisted photochemical vapor generation for the determination of lead in environmental samples by multicollector-ICPMS. Anal Chem 87:4495–4502. https://doi.org/10.1021/acs.analchem.5b00533

Gao H, Pang Y, Li L, Zhu C, Ma C, Gu J, Wu Y, Chen G (2020) One-step synthesis of the nitrogen and sulfur codoped carbon dots for detection of lead and copper ions in aqueous solution. J Sens 8828456:8. https://doi.org/10.1155/2020/8828456

Giordano MG, Seganti G, Bartoli M, Tagliaferro A (2023) An overview on carbon quantum dots optical and chemical features. Molecules 28(6):2772. https://doi.org/10.3390/molecules28062772

Gopal AR, Joy F, Dutta V, Devasia J, Dateer R, Nizam A (2024) Carbon dot-based fluorescence resonance energy transfer (FRET) systems for biomedical, sensing, and imaging applications. Part Syst Charact 41:2300072. https://doi.org/10.1002/ppsc.202300072

Hao Y, Li R, Liu Y, Zhang X, Geng L, Chen S (2023) The on–off-on fluorescence sensor of hollow carbon dots for detecting Hg^{2+} and ascorbic acid. J Fluoresc 33:459–469. https://doi.org/10.1007/s10895-022-03057-3

Hu S (2016) Tuning optical properties and photocatalytic activities of carbon-based "quantum dots" through their surface groups. Chem Rec 16:219–230

Kainth S, Goel N, Basu S, Maity B (2022) Surfactant-derived water-soluble carbon dots for quantitative determination of fluoride via a turn-off–on strategy. New J Chem 46:686–694. https://doi.org/10.1039/D1NJ04838D

Keenan JM, Zhou Y, Leblanc RM (2019) Recent Development of carbon quantum dots regarding their optical properties, photoluminescence mechanism, and core structure. Nanoscale 11:4634–4652. https://doi.org/10.1039/C8NR10059D

Kinuthia GK, Ngure V, Beti D, Lugalia R, Wangila A, Kamau L (2020) Levels of heavy metals in wastewater and soil samples from open drainage channels in Nairobi, Kenya: community health implication. Sci Rep 10:8434. https://doi.org/10.1038/s41598-020-65359-5

Li W, Hu X, Li Q, Shi Y, Zhai X, Xu Y, Li Z, Huang X, Wang X, Shi J, Zou X, Kang S (2020) Copper nanoclusters @ nitrogen-doped carbon quantum dots-based ratiometric fluorescence probe for lead (II) ions detection in porphyra. Food Chem 320:126623. https://doi.org/10.1016/j.foodchem.2020.126623

Li B, Guo X, Wang M, Liu X, Xu K (2021) A Novel, "off-on-off" fluorescent probe for sensing of F^{e3}+ and F− successively in aqueous solution and its application in cells. Dyes Pigm 194:109637. https://doi.org/10.1016/j.dyepig.2021.109637

Liu Y, Zhou Q, Li J, Lei M, Yan X (2016) Selective and sensitive chemosensor for lead ions using fluorescent carbon dots prepared from chocolate by one-step hydrothermal method. Sens Actuat B 237:597–604. https://doi.org/10.1016/j.snb.2016.06.092

Liu Y, Su X, Chen L, Liu H, Zhang C, Liu J, Hao J, Shangguan Y, Zhu G (2021) Green preparation of carbon dots from Momordica charantia L for rapid and effective sensing of p-aminoazobenzene in environmental samples. Env Res 198:111279. https://doi.org/10.1016/j.envres.2021.111279

Liu Y, Zhou P, Wu Y, Su X, Liu H, Zhu G, Zhou Q (2022) Fast and efficient "on-off-on" fluorescent sensor from N-doped carbon dots for detection of mercury and iodine ions in environmental water. Sci Total Env 827:154357. https://doi.org/10.1016/j.scitotenv.2022.154357

Liu Y, Chen L, Su X, Li W, Jiao Y, Zhou P, Li B, Duan R, Zhu G (2024) Constructing an eco-friendly and ratiometric fluorescent sensor for highly efficient detection of mercury ion in environmental samples. Enviro Sci Poll Res 31:4318–4329. https://doi.org/10.1007/s11356-023-31167-3

Long C, Jiang Z, Shangguan J, Qing T, Zhang P, Feng B (2021) Applications of carbon dots in environmental pollution control: a review. Chem Eng J 406:126848–126868. https://doi.org/10.1016/j.cej.2020.126848

Miao S, Liang K, Kong B (2020) Förster resonance energy transfer (FRET) paired carbon dot-based complex nanoprobes: versatile platforms for sensing and imaging applications. Mater Chem Front 4:128–139. https://doi.org/10.1039/C9QM00538B

Mohandoss S, Ahmad N, Khan MR, Velu KS, Palanisamy S, You S, Kumar AJ, Lee YR (2023) Nitrogen and sulfur co-doped photoluminescent carbon dots for highly selective and sensitive detection of Ag^{+} and Hg^{2+} ions in aqueous media: Applications in bioimaging and real sample analysis. Env Res 228:115898

Mohapatra S, Sahu S, Nayak S, Ghosh SK (2015) Design of Fe_3O_4@SiO_2@Carbon quantum dot based nanostructure for fluorescence sensing, magnetic separation, and live cell imaging of fluoride ion. Langmuir 31(29):8111–8120. https://doi.org/10.1021/acs.langmuir.5b01513

Molaei MJ (2019) Carbon quantum dots and their biomedical and therapeutic applications: a review. RSC Adv 9:6460–6481. https://doi.org/10.1039/C8RA08088G

Molaei MJ (2020) Principles, mechanisms, and application of carbon quantum dots in sensors: a review. Anal Methods 12:1266–1287. https://doi.org/10.1039/c9ay02696g

Pei L, Zhang W, Yang S, Chen K, Zhu X, Zhao Y, Han S (2023) Nitrogen and sulfur co-doped carbon dots as a 'turn-off' fluorescence probe for the detection of cerium and iron. J Fluoresc 33:1147–1156. https://doi.org/10.1007/s10895-022-03126-7

Podgorski J, Berg M (2022) Global analysis and prediction of fluoride in groundwater. Nature Comm 13(1):1–9. https://doi.org/10.1038/s41467-022-31940-x

Rahal M, Atassi Y (2021) Alghoraibi I (2021) Quenching photoluminescence of carbon quantum dots for detecting and

tracking the release of minocycline. J of Photochem & Photobiol A 412:113257. https://doi.org/10.1016/j.jphotochem.2021.113257
Raja S, da Silva GTST, Anbu S, Ribeiro C, Mattoso LHC (2023) Biomass-derived carbon quantum dot: "*On–off-on*" fluorescent sensor for rapid detection of multi-metal ions and green photocatalytic CO_2 reduction in water. Biomass Conv Bioref. https://doi.org/10.1007/s13399-023-04247-0
Sarkar S, Sudolská M, Dubecký M, Reckmeier CJ, Rogach ALY, Zbořil R, Otyepka M (2016) Graphitic nitrogen doping in carbon dots causes red-shifted absorption. J Phys Chem C 120:1303–1308. https://doi.org/10.1021/acs.jpcc.5b10186
Sarkar PK, Kar P, Halder A, Lemmens P, Pal SK (2019) Development of highly efficient dual sensor based on carbon dots for direct estimation of iron and fluoride ions in drinking water. Chemistry Select 4:4462–4471. https://doi.org/10.1002/slct.201900453
Shabbir H, Tokarski T, Ungor D, Wojnicki M (2021) Eco friendly synthesis of carbon dot by hydrothermal method for metal ions salt identification. Materials 14(24):7604. https://doi.org/10.3390/ma14247604
Shi Y, Xu H, Yuan T, Meng T, Wu H, Chang J, Wang H, Song X, Li Y, Li X, Zhang Y, Xie W, Fan L (2022) Carbon dots: an innovative luminescent nanomaterial. Aggregate 3(3):e108. https://doi.org/10.1002/agt2.108
Singhal P, Vat BG, Jha SK, Neogy S (2017) Green, water-dispersible photoluminescent on−off−on probe for selective detection of fluoride ions. ACS Appl Mater Interfaces 9:20536–20544. https://doi.org/10.1021/acsami.7b03346
Sisay B, Debebe E, Meresa A, Abera T (2019) Analysis of cadmium and lead using atomic absorption spectrophotometer in roadside soils of jimma town. J Anal Pharm Res 8(4):144–147. https://doi.org/10.15406/japlr.2019.08.00329
Tian J, An M, Zhao X, Wang Y, Hasan M (2023) Advances in fluorescent sensing carbon dots: an account of food fnalysis ACS. Omega 8(10):9031–9039. https://doi.org/10.1021/acsomega.2c07986
US EPA (United State Environmental Protection Agency) (2021). https://www.atsdr.cdc.gov/spl/#2019spl
Vardhan KH, Kumar PS, Panda RC (2019) A review on heavy metal pollution, toxicity and remedial measures: Current trends and future perspectives. J Mol Liq 290:111197. https://doi.org/10.1016/j.molliq.2019.111197
Wang B, Xu H, Wang D, He S (2021) The influence mechanism of HCO_3^- on fluoride removal by different types of aluminum salts. Colloids Surf: Physicochem Eng Asp J 615:126124
Wang Z, Zhang L, Zhang K, Lu Y, Chen J, Wang S et al (2022) Application of carbon dots and their composite materials for the detection and removal of radioactive ions: a review. Chemosphere 287:132313. https://doi.org/10.1016/j.chemosphere2021.132313
Wongsing B, Promkot S, Naksen P, Ouginon S, Buranachai C, Phooplub K, Jarujamrus P (2023) The development of the fluorescence-based portable device for lead (II) and formalin etermination in food samples by using nitrogen-doped carbon dots (N-CDs). J Fluoresc 33:565–574. https://doi.org/10.1007/s10895-022-03097-9
Wu H, Tong C (2019) Nitrogen- and sulfur-codoped carbon dots for highly selective and sensitive fluorescent detection of Hg^{2+} ions and sulfide in environmental water samples. J Agric Food Chem 67:2794–2800. https://doi.org/10.1021/acs.jafc.8b07176
Yadav PK, Chandra S, Kumar V, Kumar D, Hasan SH (2023) Carbon quantum dots: synthesis, structure, properties, and catalytic applications for organic synthesis. Catalysts 13:422. https://doi.org/10.3390/catal13020422
Yang F, He X, Wang C, Cao Y, Li Y, Yan L, Liu M, Lv M, Yang Y, Zhao X, Li Y (2018) Controllable and eco-friendly synthesis of P-riched carbon quantum dots and its application for copper (II) ion sensing. Appl Surf Sci 448:589–598. https://doi.org/10.1016/j.apsusc.2018.03.246
Ye Q, Yan F, Luo Y, Wang Y, Zhou X, Chen L (2017) Formation of N, S- codoped fluorescent carbon dots from biomass and their application for the selective detection of mercury and iron ion Spectrochim. Acta Part A Mol Biomol Spectrosc 173:854–862. https://doi.org/10.1016/j.saa.2016.10.039
Yoo D, Park Y, Cheon B, Park MH (2019) Carbon Dots as an effective fluorescent sensing platform for metal ion detection. Nanoscale Res Lett 14:272. https://doi.org/10.1186/s11671-019-3088-6
Zhang ZW, Shimbo S, Ochi N, Eguchi N, Watanabe T, Moon CS, Ikeda M (1997) Determination of lead and cadmium in food and blood by inductively coupled plasma mass spectrometry: a comparison with graphite furnace atomic absorption spectrometry. Sci Total Environ 205:179–187. https://doi.org/10.1016/s0048-9697(97)00197-6
Zhang X, Tan X, Hu Y (2021) Blue/yellow emissive carbon dots coupled with curcumin: a hybrid sensor toward fluorescence turn-on detection of fluoride ion. J of Haz Mat 411:125184. https://doi.org/10.1016/j.jhazmat.2021.125184
Zhu Z, Niu H, Li R, Yang Z, Wang J, Li X, Pan P, Liu J, Zhou B (2022) One-pot hydrothermal synthesis of fluorescent carbon quantum dots with tunable emission color for application in electroluminescence detection of dopamine. Biosens Bioelectron X 10:100141. https://doi.org/10.1016/j.biosx.2022.100141
Zou FR, Wang SN, Wang FF, Liu D, Li Y (2020) Synthesis of lanthanide-functionalized carbon quantum dots for chemical sensing and photocatalytic application. Catalysts 10:833. https://doi.org/10.3390/catal10080833
Zu F, Yan F, Bai XuJ, Wang Y, Huang Y, Zhou X (2017) The quenching of the fluorescence of carbon dots: a review on mechanisms and applications. Microchim Acta 184:1899–1914. https://doi.org/10.1007/s00604-017-2318-9